KSTAR POLOIDAL AND TOROIDAL FIELD DESIGN*

B.J. Lee[1], N. Pomphrey[2], C.S. Chang[3], S.Y. Cho[1], S.C. Jardin[2], G.S. Lee[1], G.H.Neilson[2], H. Park[1,2], W. Reierson[2], and KSTAR team[1,2]

[1] Korea Basic Science Institute, 52 Yeoeun-Dong, Taejeon, 305-333, KOREA
[2] Princeton Plasma Physics Laboratory, P.O.Box 451, Princeton, NJ 08543, USA
[3] Korea Advanced Institute of Science and Technology, Taejeon, KOREA

Abstract -- The Korean Superconducting Tokamak Advanced Research (KSTAR) will have superconducting magnets for both the poloidal field (PF) coils and the toroidal field (TF) coils. The physical arrangement of the PF set has 14 coils external to the TF coils. The analysis of the equilibrium flexibility of the KSTAR PF system determines the coil currents required to maintain prescribed equilibrium configurations over the desired range of operational parameters specified in I_p (q_{95}), β_N, and $\ell_i(3)$. Constraints on the plasma separatrix and the flux linkage through the geometric center of the plasma are specified for the free boundary equilibrium calculations. In order to eliminate the remaining freedoms the coil current distribution is regularized (smoothed) by minimizing the quantity $\sum_{j=1}^{ncoil} (Ij / \Delta Aj)^2$ where ΔAj is the area of each PF coil. The ripple magnitude due to the finite number of TF coils and the size of the port for the neutral beam injector determine the number, size, and shape of TF coils. Two ripple criteria for a shaped plasma are used for types of ripple transport. The current design of the TF coil, 16 coils and D-shape, is big enough to satisfy requirements on the ripple magnitude at the plasma and to provide an adequate access for tangential NB injection.

I. Introduction

KSTAR will have a poloidal field system capable of providing a flux swing of 14 Webers (Volt-Seconds) to allow full inductive operation for approximately a 20-s flattop. With superconducting toroidal and poloidal field coils and non-inductive current drive, it will be capable of true steady-state operation.

Among 7 PF coil pairs, which are up-down symmetric, the central solenoid consists of four pairs of modules (PF1 - 4) to provide some shaping capability. In addition there is a pair of divertor coils (PF5) and two pairs of outboard ring coils (PF6-7). The seven coil-pair arrangement (see Figure 1) has the ability to provide a pure Ohmic distribution so the plasma shape can be held fixed during an inductively maintained flattop. The PF coil centroid locations were scaled from their locations in the TPX design, where a detailed optimization was performed. The aspect ratios for the individual coils were chosen equal to the values assumed for TPX [1].

Table 1: PF coil specification (m)

coil	R_c	Z_c	ΔR_c	ΔZ_c	turns
PF1U(L)	0.543	±0.257	0.2148	0.514	180(180)
PF2U(L)	0.543	±0.712	0.2148	0.395	144(144)
PF3U(L)	0.543	±1.027	0.2148	0.236	90(90)
PF4U(L)	0.543	±1.264	0.2148	0.237	90(90)
PF5U(L)	1.038	±2.297	0.4000	0.400	256(256)
PF6U(L)	3.033	±1.920	0.1500	0.350	84(84)
PF7U(L)	3.915	±1.095	0.1500	0.350	84(84)

II. Flexibility of KSTAR PF system

Configuration flexibility is an important element of the KSTAR design approach. We have attained flexibility in the design by demonstrating the ability to accommodate a wide range of plasma parameters. The equilibrium flexibility of the KSTAR PF system is examined using the Tokamak Simulation Code [2] (TSC) free boundary MHD equilibrium feature, which solves the Grad-Shafranov equation for chosen plasma shape constraints and plasma profiles.

The primary purpose of these analyses is the determination of the PF coil currents required to maintain prescribed equilibrium configurations over the desired range of operational parameters, usually specified in terms of the plasma current I_p (q_{95}), normalized toroidal beta β_N $\left(\equiv \beta(\%) \dfrac{I(MA)}{a(m) B_T(T)} \right)$, and normalized plasma internal inductance $\ell_i(3)$ $\left(\equiv \dfrac{2V\langle B_p^2 \rangle}{(\mu_0 I_p)^2 R_0} \right)$ where V is the plasma volume and $\langle B_p^2 \rangle = \int B_p^2 dV / \int dV$ is the volume average of the square of the poloidal magnetic field.

* Work supported by the Ministry of Science and Technology of the Republic of Korea

0-7803-4226-7/98/$10.00 © 1998 IEEE

In order to determine the initial flux bias, two sets of PF coil currents which satisfy the shape constraints while minimizing $\sum_{j=1}^{ncoil} (Ij / \Delta Aj)^2$ (where ΔA_j is the area of each PF coil), but which differ in plasma flux linkage by 1 Weber, are calculated at each of the corners of ℓ_i - β_N operating space. The difference of these calculations is used to obtain an Ohmic distribution of currents. Then, superconductor limits on fraction of critical current density, current density in the copper stabilizer, heat transfer rate for a recovery event, and temperature headroom of superconductor are analyzed. Optimal coil currents are determined by using the Ohmic distribution to find out the preferable initial bias flux linkage. Finally we confirm that the flux surface for the plasma equilibrium with the modified currents satisfies the strike point and scrape-off-layer (SOL) flux surfaces constraints. It is necessary, size of the PF superconductor is adjusted in order to satisfy superconductor constraints.

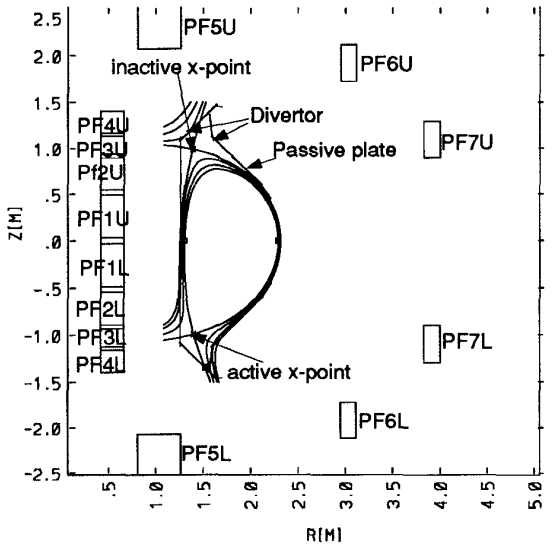

Figure 1. PF Coil Configuration in KSTAR

A. Equilibrium Description

The equilibrium analyses utilize a variety of profile forms for pressure and toroidal field function g (=RB_t) to represent nominal and extreme ranges of plasma operation. The nominal profiles have the following forms for the plasma pressure and g:

$$\frac{p(\psi)}{p(0)} = (1-\hat{\psi})^{\alpha_p}, \qquad (1)$$

and

$$g^2 = (RB_T)^2 + 2[-c_{g1}\hat{\psi}^{\alpha_g} - 4c_{g2}(1-\hat{\psi})] \qquad (2)$$

where $\hat{\psi} = \frac{\psi_{lim} - \psi}{\psi_{lim} - \psi_{min}}$ is the normalized poloidal flux.

The desired β_N is obtained by adjusting $p(0)$. Typical values of the pressure and toroidal field function shape parameters are α_p= 2.0 and α_g= 2.0. The parameters c_{g1}, c_{g2}, and α_g in the toroidal field function are adjusted to yield the desired values of ℓ_i and I_p.

B. Plasma Operating Space and Constraints

Free boundary equilibria have been generated to assess the ability of the KSTAR poloidal field system to produce equilibrium satisfying all the shape constraints for plasma profiles in the range $1.5 \le \beta_N \le 5$ and $0.4 \le \ell_i \le 1.3$ for steady-state. Also, startup reference equilibria with β_N = 0.3 and $0.8 \le \ell_i \le 1.2$ can be produced. We have also verified that Double-Null (DN) configurations with high q_a = 5 at β_N = 5 are possible.

The 14 PF coils are connected in an up-down symmetric set of seven independent circuits (PF1U+L, PF2U+L, PF3U+L, PF4U+L, PF5U+L, PF6U+L, and PF7U+L) for DN equilibria. For the DN analyses, there are typically 3 hard geometric constraints on the plasma separatrix, namely specified values for the inboard and outboard midplane radii (R ± a at Z=0), and a specified location for the separatrix strike point on the divertor plate. The flux linkage through the geometric center of the plasma is also specified, which means there are 4 strict constraints among the seven independent coil groups. The remaining 3 degrees of freedom are used to position the X-point so that the SOL surface that is 2 cm from the separatrix on the midplane does not intersect any material surfaces other than the divertor, to maintain sufficient elongation to satisfy $q_{95} > 3$, and to regularize the coil current distribution by minimizing the quantity $\sum_{j=1}^{ncoil} (Ij / \Delta Aj)^2$. Table 2 is the summary of the PF coil currents at two startup and four steady-state operating corners. Note that I_p was lowered for the ℓ_i =1.3 and β_N=5 case to satisfy the high q_{95} (>5) constraint. The PF coils for Single-Null (SN) operation are connected into 11 independently controllable circuits with PF1U+L, PF2U+L, PF3U, PF3L, PF4U, PF4L, PF5U, PF5L, PF6U, PF6L, and PF7U+L. The geometric constraints on SN plasmas are the same as on DN plasma, but in addition the inactive separatrix must be outside the +2 cm surface. Table 3 has the same information as Table 2, but for SN plasmas. High ℓ_i cases also have reduced I_p to satisfy the q_{95} > 3 constraint.

Table 2. Coil currents and flux linkages for 6 flexibility equilibria

	Startup Flexibility		Steady-State Flexibility			
β_N	0.3	0.3	1.5	1.5	5	5
$\ell_i(3)$	0.8	1.2	0.4	1.3	0.4	1.3
I_p	2 MA	2 MA	2 MA	2 MA	2 MA	1.2 MA
Flux linkage (Webers)	4.5	4.5	6	6	6	6
I_PF1(kA-turn)	-2516	-3323	-2131	-4017	-981	-2463
I_PF2(kA-turn)	-1555	64	-2492	561	-3812	-846
I_PF3(kA-turn)	874	823	-159	201	419	-482
I_PF4(kA-turn)	1670	1115	428	12	1655	-504
I_PF5(kA-turn)	2402	1757	3758	1549	3524	-211
I_PF6(kA-turn)	-1117	-74	-2989	-200	-2515	285
I_PF7(kA-turn)	-508	-1250	610	-1336	41	-1361

Table 3. Coil currents and flux linkage at four steady-state operating corners of SN plasma

	Steady-State Flexibility			
β_N	1.5	1.5	5	5
$\ell_i(3)$	0.4	1.3	0.4	1.3
I_p	2 MA	1.75MA	2 MA	1.6 MA
Flux linkage	6	6	6	6
I_PF1U(kA-turn)	-2380	-3705	-1857	-2908
I_PF2U(kA-turn)	-2162	289	-2047	-60
I_PF3U(kA-turn)	-116	-103	62	-360
I_PF4U(kA-turn)	397	-271	674	-556
I_PF5U(kA-turn)	2589	-271	2099	-987
I_PF6U(kA-turn)	-2137	546	-1321	1351
I_PF7U(kA-turn)	263	-1442	-503	-2041
I_PF3L(kA-turn)	-116	-179	62	-23
I_PF4L(kA-turn)	397	-363	674	-101
I_PF5L(kA-turn)	3909	1108	3307	365
I_PF6L(kA-turn)	-2746	-34	-1845	743

III. KSTAR TF coil design

Axisymmetry of magnetic field topology insures good classical particle confinement. However, due to discreteness of the TF coil system, it is unavoidable to have some ripple component in the toroidal magnetic field. This can allow rapid loss of energetic ions. For the ripple strength δ, we use the peak-to-average definition ($\equiv (B_{max}-B_{min})/(B_{max}+B_{min})$). Ripple strength is a function of position. We use θ to denote the poloidal angle measured from the outside midplane.

The ripple requirement to avoid energetic particle loss can give design requirements on size, shape, and number of TF coils. Two types of ripple losses are used in the KSTAR design phase: ripple trapping (RT) and collisionless stochastic ripple (CSR) losses. Collisional effects are neglected at this stage of design phase.

A. Ripple trapping loss

Weakly collisional, energetic particles can be trapped in the local ripple well if their perpendicular (to **B**) energy is much higher than the parallel energy. The ripple-trapped particles can, then, be lost rapidly by ∇B drift motion. Neutral-beam ions or ICRH-tail ions can be pitch-angle scattered into the ripple trapping region as they slow down.

$$\delta < \delta_t = \frac{a}{NqR}\frac{\sin\theta\left[\left(1+\kappa^2\right)/2\right]^{1/2}}{\left(\sin^2\theta+\kappa^2\cos^2\theta\right)^{1/2}} \qquad (3)$$

where a is the horizontal minor radius, N is the number of TF coils, q is the safety factor, R is the major radius, and κ is the elongation factor.

Local magnetic ripple well is usually maximal around the outside midplane, $\theta=0^0$. However, $\theta=0^0$ is not a good place to study a ripple-trapping requirement because any non-zero ripple value gives a local ripple well there, which may well be of measure zero. As is now common in machine design studies, $\cos\theta=0.8$ is chosen as a good reference place to set the requirement against ripple trapping. Eq (3) gives δ_t = 0.3% for KSTAR.

B. Collisionless stochastic loss

The non-axisymmetric ripple field induces stochastic radial motion of trapped ions when the ion energy exceeds a critical value characterized by the ripple strength at the banana tip. A reasonable upper limit against CRS loss of energetic ions can be obtained by requiring that the ions turning at $\theta=90^0$ are below the CRS threshold. By modifying the formula of Goldston-White-Boozer [3] to include the effect of elongation and triangularity, we have

$$\delta < \delta_s \approx \frac{\kappa}{\sin\alpha}\left(\frac{a}{\pi RNq}\right)^{3/2}\frac{0.6}{\rho q'} \qquad (4)$$

where ρ is the gyroradius of the energetic ion, α is the angle between the flux surface and the vertical line at $\theta=90^0$, and q' is the radial derivative of the safety factor. The required ripple strength for the stochastic loss is inversely proportional to the particle speed. Eq.(4) gives δ_s = 0.01% for KSTAR.

A series of calculations of the ripple due to various possible TF magnet designs were performed. Three different TF shapes were considered; D-shape, DIII-D-shape (angled D), and TPX racetrack shape. The cases of 16 and 12 TF coil

were also considered with their different sizes. AV8 code [4] was used for the calculations, with each TF coil as a toroidal array of filaments.

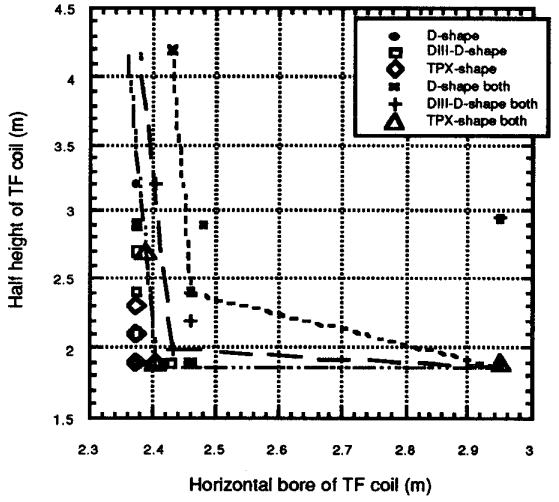

Figure 2. Racetrack shape requires the smallest TF coil

The region of the right hand and upper sides of lines in Figure 2 basically represents the height and width of TF coil which can satisfy δ_t<0.3% and δ_s<0.01%. Lines connect the points at each TF shape at which both criteria are satisfied. Other points without the label "both" satisfy only one or none of criterion. The TPX-shape gives the smallest TF coils. Overall the TF coil shape strongly affects δ. Another observation is that δ_t is more sensitive to TF width than height; δ_s is more sensitive to TF height than width.

IV. Summary

The KSTAR PF system, which has 7 up-down symmetric coil pairs, can satisfy strike-point and SOL flux surface constraints for both DN and SN plasmas if X-point position is allowed to vary. Seven and 11 independent circuits were used for DN and SN plasmas respectively to generate equilibria over the desired range of ℓ_i - β_N operating space. Superconductor allowables for PF coils are satisfied for both DN and SN.

The RT loss requirement is automatically satisfied in KSTAR because the beam port allowance demands that the outer legs of the toroidal field coils be located far away from the plasma. The CSR loss requirement, however, sets a lower bound on the number of TF coils. At least 16 TF coils are needed with reasonable height. The racetrack shape requires the smaller TF coil set than D and DIII-D shapes.

References

[1] J. Schmidt, K. Thomson, et al., J. of Fusion Energy, **12**, 221 (1993)

[2] S.C. Jardin, N. Pomphrey, and J. DeLucia, J. Comp. Phys, **66**, 481 (1986)

[3] R.J. Goldston, R.B. White, and A.H. Boozer, Phys. Rev. Lett. **47**, 647 (1981)

[4] D.K. Lee, Private communication, (1996)